

Study of Surface Raman and Fluorescence Enhancement of RhB Molecules Adsorbed on Au Nanoparticles

Jun Tang, Huanfei Wen, Penglan Chai, Jun Liu⁺,
Yunbo Shi, and Chenyang Xue

Key Laboratory of Instrumentation Science and Dynamic Measurement, Science and Technology on Electronic Test and Measurement Laboratory, North University of China, Taiyuan, Shanxi Province, China

⁺ corresponding author: liuj@nuc.edu.cn

[Submitted: May 2, 2012; revised: September 27, 2012; accepted: October 9, 2012]

Keyword: SERS; SEF; Au Nanoparticles; RhB molecules; Bio-chemical sensing

Abstract: In this work, an interesting phenomenon demonstrating the similarities between the results from both Surface Enhanced Raman Spectroscopy (SERS) and Surface Enhanced Fluorescence (SEF) for rhodamine B (RhB) molecules adsorbed on gold nanoparticles was reported. By changing the deposition time, porous Au nanoparticle films with various densities and sizes were deposited. Via thermal annealing, the densities and sizes were modified. It is concluded from the results that the intensity of SERS and SEF varied in parallel with different Au nanoparticle films: different sizes and different densities. We believe that the results obtained can provide us with a reference when developing bio-chemical sensors based on Surface Enhanced Raman Spectroscopy and Surface Enhanced Fluorescence.

1. Introduction

Owing to the unique optical and electronic properties of metallic nanoparticles such as gold and silver, a widespread interest has recently occurred which led to the development of the sensitive spectroscopic analytical techniques with the emergence of nanotechnology [1, 2]. Their applications were distributed in many new fields, one of which being bio-chemical sensors [3]. From the literature reported, it is concluded that the localized near field electromagnetic enhancement occurred in the vicinity of metallic nanoparticles can be applied to improve the sensitivity of different optical techniques as Surface Enhanced Raman scattering (SERS) [4,5] and surface enhanced fluorescence (SEF) [6]. It is also reported that the gold nanoparticles can act as a very efficient quenching for fluorescent dyes, theorized to be due to the fluorescence resonance energy transfer from the dye molecules to gold nanoparticles [7, 8]. However, the relative definite reason of those effects is still unclear and a Raman and Fluorescence enhancement has been observed for molecules indirectly contacting with silver nanoparticles [9].

SERS and SEF are two promising techniques for the study of molecular detecting in biology [10]. It was in the mid-1980s when fluorescence enhancement from colloidal surfaces was first reported [11, 12]. In recent years the demand for detecting extremely low concentrations of molecules of biological interest or even the detection of single molecule signatures has increased the interest in enhanced fluorescence and Raman spectroscopy. The electromagnetic enhancement in both SERS and SEF is caused by localized surface plasmons at the surface of metallic nanoparticles, so the manufacture of metallic nanostructured substrates using chemical or physical methods is essential.

In this paper, we report some interesting phenomena, such as common changes of both Raman and luminescence enhancement for rhodamine B (RhB) molecules adsorbed on gold nanoparticles. A gold nanoparticle substrate was applied using DC magnetron sputtering, an efficient and low cost deposition method. Au nanoparticle films were deposited on P-doped silicon or thermal SiO₂ substrate on silicon wafers and, due to the different deposition times, substrates with different density and sizes of Au nanoparticles were fabricated. With the comparative analysis of different substrates, the variation of both Raman and luminescence spectrum appeared to change in similar

manners. It suggests that the SERS and SEF have a common electromagnetic enhancement mechanism. By adjusting the parameters such as density and size, the performance of sensors based on Au nanoparticles can be optimized. We believe that the results obtained can provide us with a reference when developing bio-chemical sensors based on SERS and SEF.

2. Experimental

P-type silicon wafers and 1 μm thick thermal SiO_2 on Si were used as the substrate. The purity of gold target is 99.99%. Solutions with 10^{-4} mol/l RhB were prepared by adding 0.479 mg of RhB to 10 mL of deionized (DI) water.

The substrates were cleaned ultrasonically with acetone and ethanol for 5 minutes, rinsed with DI water, and dried by Nitrogen. Au nanoparticle films were deposited by DC magnetron sputtering. The films were prepared with the substrate holder positioned at 70 mm from the Gold target. The pressure was set to about 20 mbar and a DC current on the Au target was 20 mA. The deposition time was 1 min, 2 min, 4 min, and 6 min. The samples were removed after a 2 hour immersion into a 10^{-4} mol/l solution of RhB in DI water. In addition, the samples were dried prior to the acquisition of the spectra before testing.

The SERS and SEF characterizations were recorded on a RENISHAW Invia Raman Microscope System. The 514.5 nm laser line of an Ar⁺ laser was used. In order to minimize heating and photo bleaching effects, the laser power was 5.0 mW. Spectrum intensity calculations were performed with the assistant of PeakFit (v4.12).

Thermal annealing (OTF-1200X) was used to treat samples after the sputtering process. Nanoparticle topography characterization studies were performed with a Scanning Electron Microscope (SEM, JSM-7001F, Japan) and an Atomic Force Microscope (AFM, CSPM-3400, China). The AFM measurement results presented in this paper were recorded under tapping mode. The nanoparticle size and density calculations were performed with the assistance of IMAGER (Ver. 4.60). Due to the lateral enlargement of the AFM measurements for the nanoparticles, the diameters of the nanoparticles calculated in this paper were mainly from the heights of the nanoparticles.

3. Results and Discussion

3.1 SERS and SEF of the nanoparticle films with different deposition times

In this part, thermal SiO_2 on Si was used as the substrate. To have a clear understanding of the RhB molecules adsorbed on gold nanoparticles, both the photoluminescence (PL) and the Raman spectrum of the RhB on Au nanoparticles were measured. The RhB was applied through incubation of the substrates in 10^{-4} mol/l solution of RhB in water and the solution on substrate was dried before the acquisition of the Raman and fluorescence spectra. The samples were excited by the 514.5 line of an Argon ion laser. Raman and photoluminescence measurements were performed respectively in the region of 400 cm^{-1} - 1700 cm^{-1} and 525-850 nm.

Different deposition times were used to study the parameter's affect of the RhB molecules adsorbed on gold nanoparticles: 1 min, 2 min, 4 min, and 6 min. This data is shown in Figure 1(a) and (b) and presents the Raman and PL spectra of the RhB on the Au nanoparticles with different deposition times. From the calculated intensity variations of the Raman and PL spectra, it can be concluded that, with the increase in deposition time, a clear increase of both Raman and PL intensity was observed, as shown in Figure 1 (c) and (d). For the Raman spectrum, such as the Raman peak of 1650 cm^{-1} , the intensity increased from $1,678\pm 45$ (a.u.) in the beginning 1 min to $22,788\pm 1536$ (a.u.) at the deposited time of 4 min, corresponding to a 13.58 fold of intensity increasing. After a certain level, however, the increased deposition time caused the intensity to decrease. On the whole, the trend of changes of Raman intensity increased gradually at first and then decreased.

Meanwhile, it seemed to have three bands present centered at peak 1, 2 and 3 for the PL intensity, as shown in Figure 1(b). The intensity of the peak 2 increased from 4,640 (a.u.) initially to 25,009 (a.u.) for a deposition time of 2 min. Then, the intensity decreased after 2 min for PL. It was found

that the trend of changes of PL intensity increased gradually at first and then decreased, which is similar with the trend of Raman intensity. As shown in Figure 1 (e), the fluorescence peak also varied with the different deposited time.

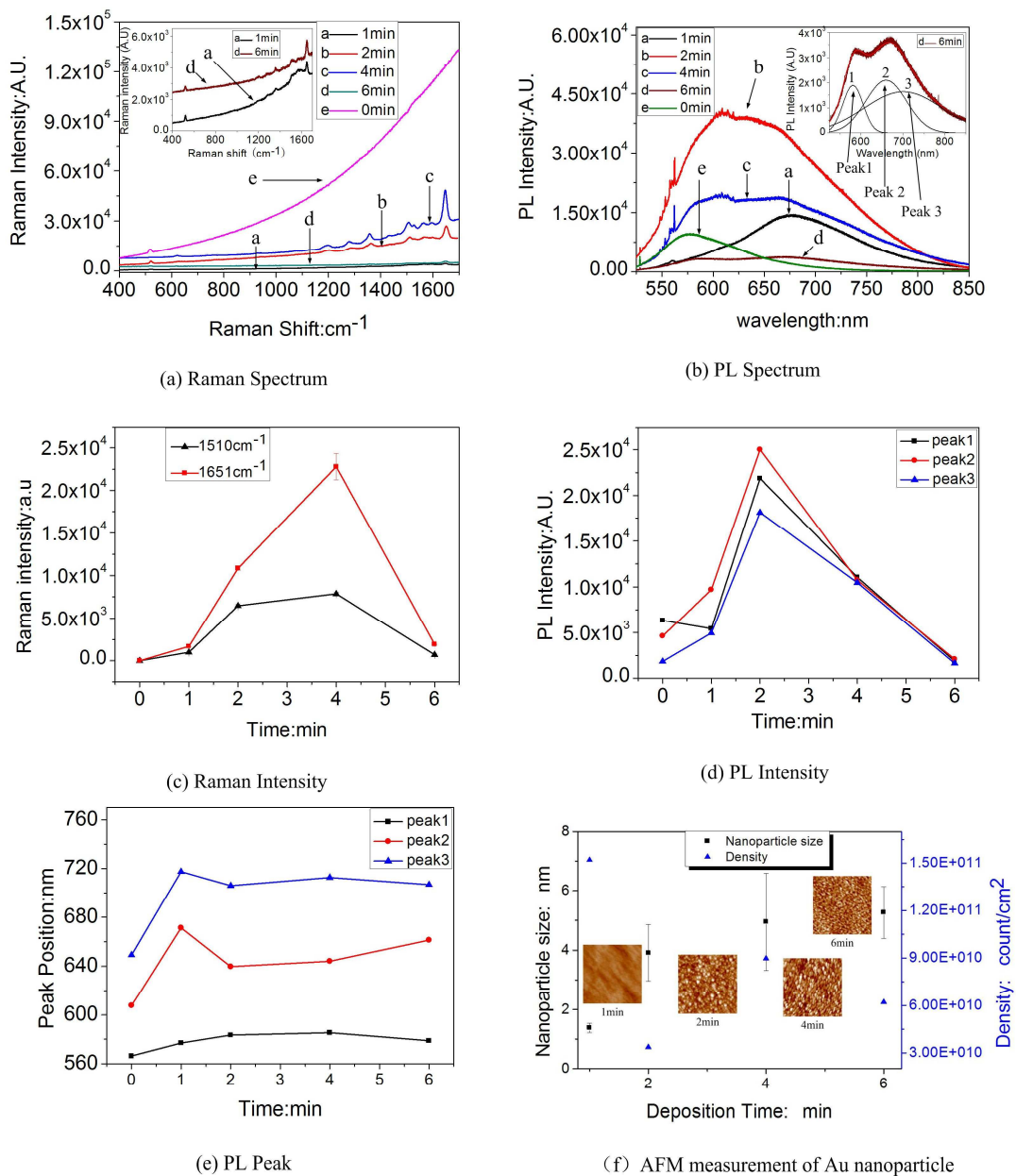


Figure 1 Raman and PL spectrum of the Au nanoparticles (on SiO₂) and AFM measurement of Au nanoparticle size and density with different deposited time.

We believe that both the variations of Raman and PL spectrums were mainly caused by the changes of both nanoparticle size and density when the deposition times were increased. Through the testing with AFM, we obtained that the mean sizes were 1.38 ± 0.16 nm, 3.91 ± 0.95 nm, 4.95 ± 1.64 nm, and 5.26 ± 0.87 nm for the deposited times of 1 min, 2 min, 4 min, and 6 min, respectively, and the densities were $1.52 \times 10^{11}/\text{cm}^2$, $3.37 \times 10^{10}/\text{cm}^2$, $8.99 \times 10^{10}/\text{cm}^2$, $6.22 \times 10^{10}/\text{cm}^2$, respectively, as shown in Figure 1 (f). A clear increase in nanoparticle size was observed.

It is concluded from the literature that the final electromagnetic enhancement strongly depends on the size, shape, and distribution of metallic nanostructure [13]. The mechanism of SERS is of electromagnetic nature and related to localized surface plasmons (LSP) [14]. When a surface plasmon is confined to a particle of a size comparable to the wavelength of light, that is, a nanoparticle, the particle's free electrons participate in the collective oscillation, and it is termed as

a localized surface plasmon [15]. This mechanism enhances the whole of the molecular Raman scattering peaks. At the beginning, for the smallest particles, localized surface-plasmon resonance extinction is dominated by absorption. So the intensity of Raman is very small at the deposition time of 1 min and as particle size increases, scattering takes over. At the same time, the AFM image of Figure 1 (f) clearly shows that the nanoparticle film has a rather porous structure. Extremely intense local electromagnetic fields generated in the gaps between adjacent Au nanoparticles can strongly enhance the Raman scattering of probe molecules located in the gaps between the closely spaced Au nanoparticles. It appears that the recorded enhancement during the present experiments is of electromagnetic nature.

The sharp increase around 4 min deposition can also be related to optimum concentration of Au nanoparticles available to RhB molecules while the observed decrease for longer depositions can be attributed to the absorbance of the Raman signal by the Au nanoparticle layer itself.

The wavelength position of fluorescence peak 2 varied from 607 nm to 671 nm for the Au nanoparticles substrate after a 1 min deposition. We surmise that in this case, when the density of the nanoparticles is small, the luminescence originates from RhB molecules adsorbed at the SiO₂ substrate. The luminescent molecules are adsorbed at the Au nanoparticles for longer depositions. We attribute the observed red shift to surface plasmon resonance (SPR), as discussed by Mafune [16]. The effect of including the particulate modification of externally incident light is to increase the scattering cross section at some wavelengths. The local field is enhanced due to interference of the incident and reflected light while the over effect is a shift in the position of the enhancement peaks [17].

The changes of the fluorescence peak intensity matched the changes of the Raman intensity for the various substrates prepared. The parallel evolution of Raman and fluorescence intensity with Au nanoparticles becomes more prominent as the density of the Au nanoparticles increases. The phenomenon should be useful for application in the bio-chemical sensor region.

The other mechanism is characterized by the charge transfer from the Au nanoparticles to the RhB molecules and back. The charges transferred change the electronic structure of the dye molecules adsorbed on the Au nanoparticles, resulting in the increase of Raman and PL intensity.

3.2 Effect of the substrate materials

We have next investigated the substrate effect on the RhB molecules adsorbed on Au nanoparticles under chemical solutions. P-doped silicon containing a resistivity of about 7 to 12 Ω .cm was used as the substrate. With the same experimental conditions, we deposited the Au nanoparticles with different deposition times. Due to the different deposition time, the density and size differed with each other. The mean sizes were 2.43 ± 0.15 nm, 4.28 ± 1.03 nm, 5.43 ± 0.64 nm, and 6.19 ± 1.95 nm for the deposition times of 1 min, 2 min, 4 min, and 6 min, respectively, while the mean densities were $8.24 \times 10^{11}/\text{cm}^2$, $9.44 \times 10^{10}/\text{cm}^2$, $1.43 \times 10^{11}/\text{cm}^2$, and $5.88 \times 10^{10}/\text{cm}^2$, respectively. This information is shown in Figure 2 (f). The average size and the density of nanoparticles deposited on Si substrate were larger than the nanoparticles deposited on SiO₂ substrate for deposition times shorter than 6 min. That is because the nanoparticles tend to gain one excess electron in the process of sputtering, which allows the nanoparticles to be electrostatically manipulated. P-type Si provides the positive charges on the surface of the Si substrate and also provides the electrostatic interactions with negatively charged gold nanoparticles.

With the varying of density and size, the Raman and PL spectra were recorded and the intensity variations were concluded as it is shown in Figure 2. From the results, it can be concluded that for the silicon substrate, both the Raman and PL intensity were much weaker, compared with the intensity on the SiO₂ substrate. Also, the variations of the intensity were much smaller, with 1.55 and 3.3 fold of variations for the Raman peak of 1650 cm^{-1} and PL peak 2, respectively. Similarly, the whole trend of changes of Raman and PL intensity increased gradually initially and then decreased. The highest intensity was at the deposition time of 4 min and 2 min for Raman and PL spectra, respectively. Also, the fluorescence peak varied with the different deposition times.

According to Surface Plasmon Resonance Modes reported by *Ergun Simsek* [18], the substrate (Si or SiO₂) having different refractive indices affect the relative intensity of SERS and SEF signals.

We observed that RhB molecules adsorbed directly on Si substrate exhibits weaker fluorescence than SiO_2 substrate. It also reveals that the fluorescence intensity was quenched when the RhB molecules adsorbed on Si substrate.

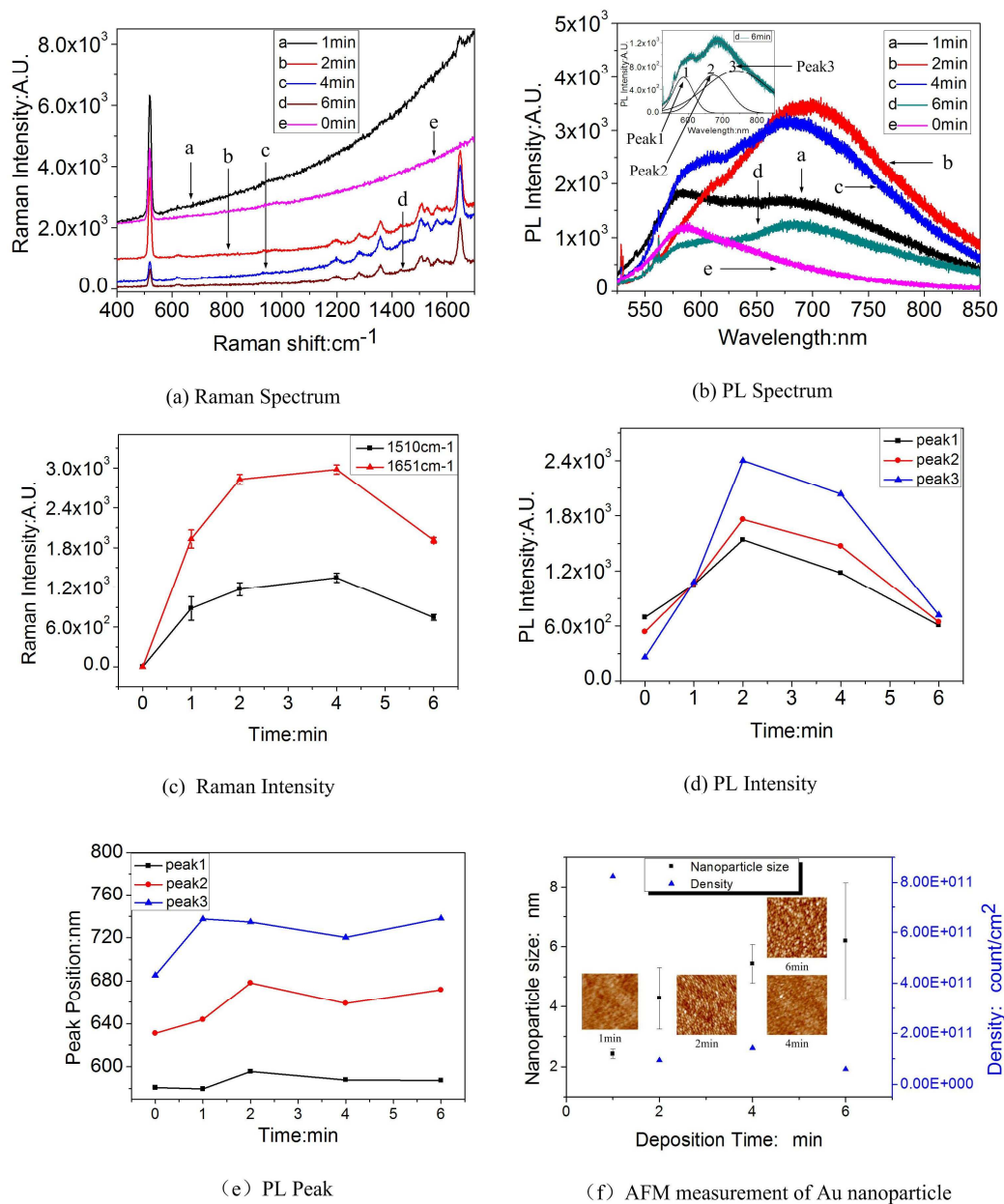


Figure 2 Raman and PL spectrum of the Au nanoparticles (on Si) and AFM measurement of Au nanoparticle size and density with different deposited time.

In addition, we can surmise that the interaction between nanoparticles and substrates affect the SERS and SEF intensity of RhB molecules through the comparative analysis of different adsorption substrates. Similarly, the trend of change of the fluorescence peak intensity followed the variation of the Raman intensity for the various substrates prepared.

3.3 Effect of the nanoparticle film thermal annealing

In order to further understand how the RhB molecules adsorb on Au nanoparticles, we investigate the role of thermal annealing to the Au nanoparticle films. Au nanoparticles deposited on SiO_2 substrate were used in this study and the deposited time was 2 min. Four same samples were thermally annealed at different temperatures 300°C , 400°C , 500°C and 600°C , respectively by using a conventional furnace (OTF-1200X) in an air environment for 2h. When the furnace reaches the appropriate temperature, the sample was placed in furnace. The furnace was turned off after 2 h

later and the sample was removed. In other words, the morphology of Au film was further modified by mean of annealing. The samples were taken out after 2 hours immersion into a 10^{-4} mol/l solution of RhB in DI water.

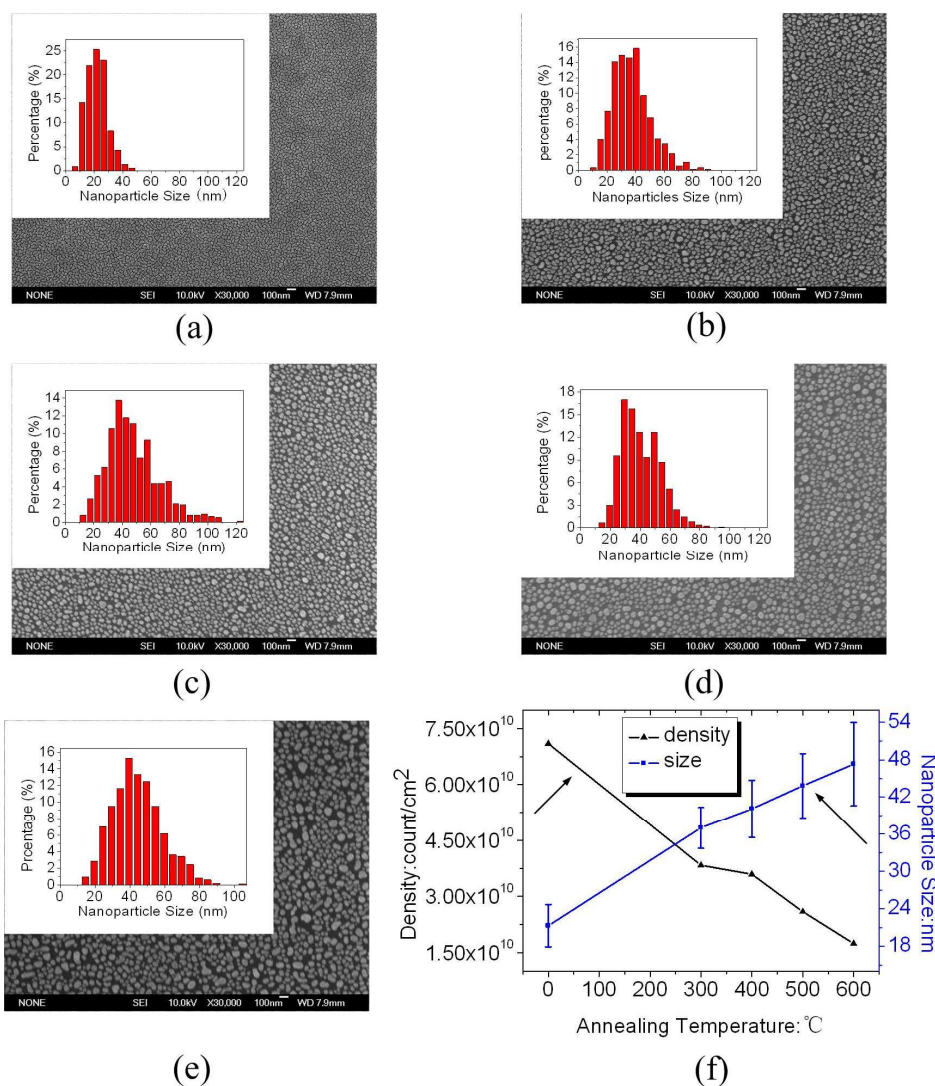


Figure 3 FESEM measurement results of the Au nanoparticles size and density evolution with different annealing temperature.

As showed in Figures 3 (a)-(e), SEM was employed to determine the size of nanoparticles and their distribution. The Au nanoparticle's size and density were calculated, as shown in Figure 3 (f). From the measurement results, it can be concluded that the mean size increased from 21.3 ± 3.4 nm to 47.3 ± 6.7 nm with the increase of the annealing temperature, while the density decreased from $7.1 \times 10^{10} / \text{cm}^2$ to $1.74 \times 10^{10} / \text{cm}^2$.

High-temperature annealing of Ag film deposited onto a smooth dielectric substrate has shown to yield self-organization of metal clusters on the film surface [19]. The surface tension caused the metal atoms of thin films to coalesce together to form the particles at high temperature. Here the self-assembly of Au film took place at the different annealed temperature and existed in the different form of morphology as the above calculation of the size and density.

Corresponding to the annealing treatment, the PL and Raman spectrum of the annealed Au nanoparticles were performed. From the intensity variations of the PL and Raman spectra, it can be concluded that, for the Raman spectra, such as the peak of 1650 cm^{-1} , the intensity increased from 11242 ± 1651 (a.u.) in the at first to 61567 ± 2670 (a.u.) at the 500°C , then intensity decreased to 46564 ± 1593 (a.u.) at 600°C , as it is shown in Figure 4. For the PL spectrum peak 2, the highest intensity reached at 300°C . Both Raman and PL intensity kept a similar trend that increased first and decreased later.

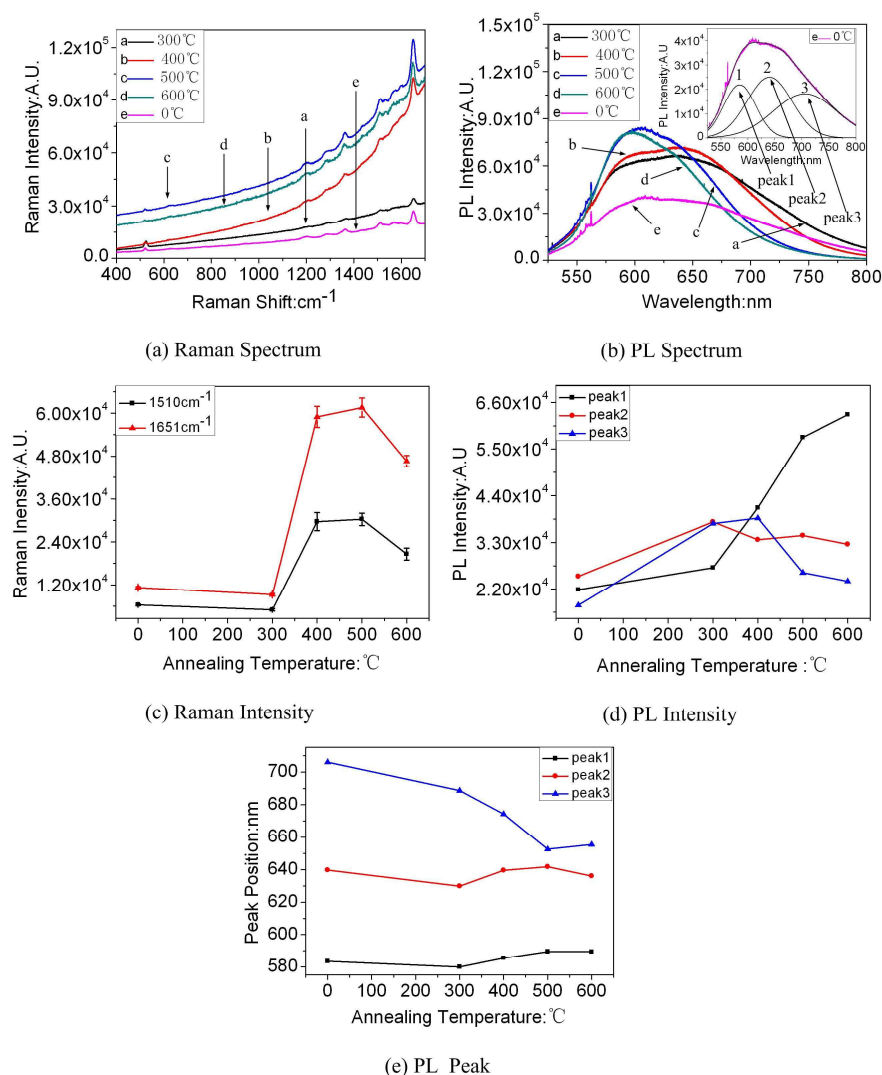


Figure 4 Raman and PL spectrum of the Au nanoparticles (on SiO₂) with different annealing temperature.

Theoretically, this effect is related to surface plasmon resonance. It can be attributed to the enhancement of the local electromagnetic field near the metal surface when the wavelength of the irradiation source is coincident with the optical absorption of the surface plasmon [20]. LSP are collective oscillations of the conduction electrons in metal particles and movement of these conduction electrons acts as a restoring force, allowing a resonance to occur at a particular frequency, which is termed as the Surface Plasmon Resonance (SPR).

However, localized surface plasmon resonance depends on the size of the nanoparticles and environmental variables, so the effect of SERS and SEF is related in the same way. It was found that with modification of the annealing treatment, the morphology of Au nanoparticles is likely to be beneficial for the effect of SERS and SEF. We found that there was a maximum effect of SERS and SEF intensity for our samples, at the size of 43.8 ± 5.2 nm and 40.1 ± 4.6 nm, respectively for the annealed samples. Through the analysis of the experiment above, we believe that the experimental results can provide us with a reference while optimizing the properties of sensors based on SERS and SEF.

4. Conclusions

Au nanoparticles were fabricated on different substrates by sputtering, an efficient and cost-effective method. The morphology of the Au nanoparticles varied with the different deposition times and through having a rapid thermal annealing treatment. The substrates were modified

through 2 hour immersion into a 10^{-4} mol/l solution of RhB in DI water. With the test of Raman and luminescence spectra, the properties of samples were investigated and we have observed strong similarities in the trend of changes of Raman and luminescence enhancement intensity from RhB molecules adsorbed on the Au nanoparticles.

Furthermore, there was an optimal morphology and size of Au nanoparticles corresponding with a maximum effect of SERS and SEF. For the first experiment, the maximum effect of SERS and SEF intensity was at the deposition time of 4 min and 2 min, respectively. From the discussion of RhB molecules spectra above, the control of gold nanoparticles morphology can adjust the spectrum of RhB molecules. Although the mechanism of this phenomenon is still not clear, we believe that the results reported in this paper can provide a reference for the metal nanomaterial exposed to biochemical solutions when we are developing low-cost biochemical sensors.

Acknowledgments: This project is supported by the National Nature Science Foundation of China (91123016; 51105345), Nature Science Foundation of Shanxi Province (2011021016).

References:

- [1] M. Alvarez, T. Khoury, T. Schaaff, N. Shafigullin, I. Vezmar, and L. Whetten, Optical Absorption Spectra of Nanocrystal Gold Molecules, *J. Phys. Chem. B*, 1997, 101 (19), 3706–3712.
- [2] P.G. Etchegion, L.R. EC, M. Meyer, An analytic model for the optical properties of gold, *J. Chem. Phys.*, 2006, 125, 164705-164701.
- [3] L. Han, J. Luo, N. Kariuki, M.M. Maye, V.W. Jones, C.J. Zhong, Novel Interparticle Spatial Properties of Hydrogen-Bonding Mediated Nanoparticle Assembly, *Chem. Mater.*, 2003, 15, 29-37.
- [4] R.F. Aroca, *Surface-Enhanced Vibrational Spectroscopy*, Wiley, Chichester, 2006.
- [5] K. Kneipp, H. Kneipp, I. Itzkan, R.R. Dasari, M.S. Feld, *Ultrasensitive Chemical Analysis by Raman Spectroscopy*, *Chem.Rev.*, 1999, 99, 2957-2975.
- [6] E. Fort, S. Gresillon, *Surface-Enhanced Fluorescence*, *J. Phys. D: Appl. Phys.*, 2008, 41, 013001.
- [7] R.C. Powell, Thermal and Sample-Size Effects on the Fluorescence Lifetime and Energy Transfer in Tetracene-Doped Anthracene, *Phys. Rev., B* 1970, 2, 2090–2097.
- [8] T. Förster, Transfer Mechanisms of Electronic Excitation Energy, *Phys.Chem.*, 1959, 326.
- [9] K. Ray, R. Badugu, J.R. Lakowicz, Distance-Dependent Metal-Enhanced Fluorescence from Langmuir-Blodg.
- [10] X. Han, B. Zhao, Y. Ozaki, Surface-Enhanced Raman Scattering for Protein Detection, *Anal. Bioanal. Chem.*, 2009, 394, 1719-1727.
- [11] A. Leitner, M.E. Lippitsch, E. Draxler, M. Rigler, F.R. Aussenegg, Fluorescence Properties of Dyes Adsorbed to SILVER Islands, Investigated by Picosecond Technique, *Appl. Phys. B:photophys. Laser Chem.*, 1985, 36, 105.
- [12] F.R. Aussenegg, A. Leitner, M.E. Lippitsch, H. Reinish, M. Rigler, Novel aspects of fluorescence lifetime for molecules positioned close to metal surfaces, *Surf. Sci.*, 1987, 139, 935.
- [13] A. Merlen, F. L. Labarthe, E. Harte, Surface-Enhanced Raman and Fluorescence Spectroscopy of Dye Molecules Deposited on Nanostructure Gold Surfaces, *J. Phy. Chem C*, 2010, 114, 12878-12884.
- [14] A. Campion, P. Kambhampati, Surface-Enhanced Raman Scattering. *Chem. Soc. Rev.*, 1998, 27, 241-250.
- [15] K.M. Mayer, J.H. Hafer, Localized Surface Plasmon Resonance Sensors, *Chem.Rev.*, 2011, 111, 3829.

-
- [16] F. Mafune, J. Kohno, Y. Takeda, T. Kondow, Formation and Size Control of Silver Nanoparticles by Laser Ablation in Aqueous Solution, *J. Phy. Chem.*, 2000, 104, 9111.
- [17] K.C. Lee, S.J. Lin, C.H. Lin, C.S. Tsai, Y.J. Lu, Size effect of Ag nanoparticles on surface plasmon resonance, *Surf. Coat. Technol.*, 2008, 202, 5339-5342.
- [18] E. Simsek: On the Surface Plasmon Resonance Modes of Metal Nanoparticle Chains and Arrays, *Plasmonics*, 2009, 4, 223–230.
- [19] A. Feofanov, A. Ianoul, E. Krukov, S. Maskevich, G. Vasiliuk, L. Kivach, I. Nabiev, Nondisturbing and Stable SERS-Active Substrates with Increased Contribution of Long-Range Component of Raman Enhancement Created by High-Temperature Annealing of Thick Metal Films, *Anal Chem.*, 1997, 69,3731-3740.
- [20] H.G. Craighead, A.M. Glass, Optical absorption of small metal particles with adsorbed dye coats, *Opt. Lett.*, 1981, 248-250.